

**CARACTERÍSTICAS ESPACIO-TEMPORALES
DE LA PRODUCCIÓN FOTOVOLTAICA EN EL
ÁREA EURO-MEDITERRÁNEA: ANÁLISIS
CLIMÁTICO**

CLAUDIA GUTIÉRREZ ESCRIBANO

CONTENTS

Contents	i
I Introduction	1
1 Introduction	3
1.1 A changing world	3
1.2 Renewable Energies	3
1.3 Links between climate and renewable energy	3
1.4 Photovoltaic Energy	3
1.5 Resource assessment	3
1.6 Climate change and the Mediterranean area	3
1.7 General scientific question: spatiotemporal behaviour of solar resource and photovoltaic production	3
1.8 Organization of the manuscript	3
2 State of knowledge	5
2.1 Intermittency of PV	5
2.2 Variability sources in PV	5
2.3 From short to long term issues	5
2.4 Climate Change perspectives for solar resource and photovoltaic potential	5
II Data & Methods	7
3 Data	9
3.1 Solar radiation measurements	9
3.2 Satellite data	9
3.3 Modelling solar radiation	9
3.4 photovoltaic production data	9
4 Methods	11
4.1 Clustering algorithm applied to climate data	11
4.2 Simulating a photovoltaic system	13
4.3 Regional Climate Modeling simulations	16
4.4 Future projections and scenarios	16
III Results	19
5 Long-term characteristics of solar resource over the Iberian Peninsula	21

5.1 Introduction 24

Abstract

Resumen de la tesis

Part I

Introduction

INTRODUCTION

- 1.1 A changing world**
- 1.2 Renewable Energies**
- 1.3 Links between climate and renewable energy**
- 1.4 Photovoltaic Energy**
- 1.5 Resource assessment**
- 1.6 Climate change and the Mediterranean area**
- 1.7 General scientific question: spatiotemporal behaviour of solar resource and photovoltaic production**
- 1.8 Organization of the manuscript**

STATE OF KNOWDLEGE

2.1 Intermittency of PV

2.2 Variability sources in PV

2.3 From short to long term issues

2.4 Climate Change perspectives for solar resource and photovoltaic potential

Part II

Data & Methods

CHAPTER 3

DATA

3.1 Solar radiation measurements

3.2 Satellite data

3.3 Modelling solar radiation

3.4 photovoltaic production data

METHODS

4.1 Clustering algorithm applied to climate data

In a data-driven world, **pattern recognition** is being applied to many disciplines, from biology to finance or social science, to extract relevant information from the different datasets. These techniques help to understand relationships that are difficult to extract at a first sight, either due to the volume of the data, or the complexity of those relationships and the amount of different variables involved. Behind all the pattern recognition methods rely the simple fact of classify objects into similar classes.

Depending on the a priori information about the data, it is possible to apply a supervised data classification/pattern recognition or unsupervised pattern recognition.

In the first stage of a supervised pattern recognition analysis there is the ability to set the measurements that will define similarity between objects, meaning the definition of the features from the dataset. The classification of different objects in the pattern recognition analysis is implemented through these features and its selection. After that, a criteria to optimally divide the features into classes is decided and applied to them. This stage is called the classifier stage and its complexity increases with the dimensionality of the data.

However, if the similarity measurements can not be defined first, due to unknown previous labeled data, another approach will be implemented. In that case, the task will consist in identifying the similarities afterwards, from a dataset of features, applying clustering algorithms for that purpose.

4.1.1 Clustering algorithms

It is not under the scope of this work to analyse in detail all the clustering methods available, due to the vast number of them and its increasing complexity. However, it is worth it to give an overview of its classification and application in order to better understand the choice made in the study of our problem.

There are different types of clustering algorithms based on its application and the criteria to construct the clusters. The two main categories are divided in **hierarchical** and **non-hierarchical algorithms**, but there are other taxonomies based on the algorithm construction that can be used to classify different methods [ref].

The **hierarchical clustering algorithms** create a number of nested clusters and can be also divided itself in agglomerative or divisive. The first one, obtain a smaller number of cluster in each step, whereas the divisive algorithms, works on the other direction.

Most of these hierarchical algorithms are variants of the single-link or complete-link algorithms. They have a different way to measure similarity. In the first case, the distance between two clusters is the minimum of all the pairwise distances measured between the objects of the two clusters, in contrast, for the complete-link algorithm the distance is considered the maximum of all the pairwise distances.

On the other hand, the non-hierarchical or **partitional clustering algorithm**, create a number of non-overlapping clusters. These methods could be useful when the amount of data involved is large and the construction of a dendrogram, produced by the hierarchical algorithm could be computationally expensive.

The partitional methods create the group of clusters using an **optimization function** which defines the similarity. The main inconvenient of these algorithms is the in advance definition of the number of clusters. Usually, the algorithm is implemented several times for a wide number of partitions and the optimum number of clusters is defined afterwards using validity indexes criteria.

[Añadir algo más sobre algoritmos partitional](#)

4.1.2 Clustering climate data

As previously commented, the use of pattern recognition and in particular, the clustering analysis, has been widely used across many different disciplines. The use of these techniques to group together atmospheric variables that could help in environmental classifications is a more recent research field.[ref]

Historically, the climatic divisions were based mostly on the differences in vegetation types around the globe. The Koppen-Terawata classification [ref] is the most widely known climate classification and bases its divisions in obtaining the vegetation thresholds from precipitation and temperature data. Some authors had already pointed the limitations of this classifications, mostly due to two aspects: the first one is that vegetation thresholds are not well defined and that could be an issue when higher resolution spatial scales want to be defined. On the other hand, is the fact that not only precipitation and temperature are influencing the vegetation species but also other atmospheric variables, like solar irradiation, but also other environmental factors that could be related to antropogenic emissions or waste.

[Buscar más biblio de esto](#)

As these classical division are not adapted to the necessities of different fields and could be even biased, another way to geo-spatial classification is needed. In this sense it has become frequent to successfully use data-driven classification of different variables if it is necessary to give an spatially resolved answer. [ref]

4.1.3 Applied clustering method

In this work a clustering method is applied to classify solar irradiation due to the fact that classical climate division are only based on temperature and precipitation. The spatial pattern that could be extracted from the Koppen-Terawata classification, can not be used for our purpose.

A partitional commonly used clustering method has been selected to classify solar irradiation of the area. The '**k-means**' algorithm is easy to implement, due to the fact that it has been largely used over the literature.

Moreover, the combination of a **principal component analysis** of the dataset previous to the k-means algorithm application has been proved to be an useful tool to reduce the data-dimensionality and apply the algorithm in a more efficient manner.

K-Means algorithm

The k-means algorithm is a partitional clustering method that provide a set of partitions from the application of an optimization function, usually the euclidean distance. The algorithm initiates from a pre-defined number of clusters, 'k', and randomly selects a group of centroids equal to the number of clusters. The optimization function is applied to assign each object to one of the clusters, depending on the similarity (distance) to each of the centroids. This process is applied until the algorithm converges.

One of the limitations of these method is its dependency on the first selection of the centroids, that could lead to a local optimum instead to a global optimum. To solve these difficulty, the algorithm can be run many times to test the sensitivity of the algorithm to a different initial conditions. Another option is to use an initialization technique to select the centroids.

continuar

Principal Component Analysis

The Principal Component Analysis, PCA [ref], consists in a decomposition of the dataset into a number of vectors whose linear combination represents the original data. The transformation of the original data into a lower dimensional space is a reduction of the dimensionality retaining the maximum of the data variance.

The new orthogonal system has in its first coordinate axis, the projected values of the original data that preserve most of the variance in the dataset, and it is called the principal component. The rest of principal components decrease the amount of variance explained consecutively.

The PCA has been applied in advance to K-means clustering algorithm among the literature [ref]. It was explained by [ref] that the reduction in dimensionality is directly linked to K-means due to the fact that the clustering membership indicators are actually the eigenvectors given by the PCA. For this reason, it has been applied before the K-means algorithm fastening the algorithm.

Validity Index

Initialize K-Means

4.2 Simulating a photovoltaic system

In order to estimate the amount of energy produced by a photovoltaic system it is necessary first to assess the amount of energy that reach the generator surface (plane of array irradiation, $G(\alpha, \beta)$) and after this estimation, which it is not straightforward unless it is measured, the different components of the generator has to be modeled.

For the evaluation of the photovoltaic **energy yield**, defined as the amount of energy produced by a photovoltaic system divided by its nominal power, along this work we use the process explained below, which can be summarized in two steps:

1. To calculate the **effective irradiation**, $G_{eff}(\alpha, \beta)$, which is the effective irradiation after subtract optical losses, due to reflection, angle of incidence or dirtiness. The assessment of this variable has to be done from the global irradiation at the surface, $G(0)$, that can be obtain from measurements, atmospheric models or satellite datasets.
2. The second step consists in simulate the **electrical performace** of the system and estimate the power from the generator. The whole photovoltaic system includes the generator, the inverter and the transmission elements and wires.

All the processes involved in the stage of simulating a photovoltaic system in this thesis have been made using solar [ref], an R package that implements all the necessary functions to estimate the energy provided by the sytem.

4.2.1 Global effective irradiation

Assessing the amount of energy reaching cells of the photovoltaic generator requires to compute trackers movements, as well as the relative position between sun and panels throughout the year, a detailed description of these methods can be found in Perpinan.Marcos.ea2013. Once these equations are computed, the procedure is described below:

- First, global irradiation on the horizontal plane is decomposed in two components, **direct** and **diffuse** irradiation, Eq.4.1. To estimate these quantities it is necessary to consider equations proposed by [Liu1960] to characterize solar irradiation. Definition of *clearness index*, Eq.4.3, is the ratio between global irradiation and extra-terrestrial irradiation at the horizontal plane. They also proposed to relate that index with the *diffuse fraction*: the ratio of diffuse to global irradiation in Eq.4.2. This relation varies depending on the time scale. For daily values, we estimate correlation between the clearness index and the diffuse fraction using equations in [Aguiar1992]. After that, the diffuse component is obtained with the definition of the *diffuse fraction*, Eq.4.2.

$$G_d(0) = B_d(0) + D_d(0) \quad (4.1)$$

$$F_{D,d} = \frac{D_d(0)}{G_d(0)} \quad (4.2)$$

$$K_{Td} = \frac{G_d(0)}{B_{0d}(0)} \quad (4.3)$$

- Secondly, daily irradiance has to be estimated from irradiation values. Considering low variability of solar irradiance, it is assumed that average irradiance in a short interval coincides with irradiation in that interval. Regarding equations proposed by [Aguiar1992], the ratio of the diffuse irradiance to diffuse irradiation is assumed to be equivalent to the ratio of extraterrestrial irradiance to extraterrestrial irradiation Eq.4.4, and the ratio of global irradiance to daily global irradiation is followed from the same reference Eq.4.5.

$$r_D = \frac{D(0)}{D_d(0)} = \frac{B_0(0)}{B_{0d}(0)} \quad (4.4)$$

$$r_G = \frac{G(0)}{G_d(0)} = r_D \cdot (a + b \cdot \cos(\omega)) \quad (4.5)$$

- The third step considers only geometrical criteria to compute the direct and diffuse irradiance components at the inclined plane. Diffuse irradiance is calculated with the anisotropic model proposed in [hay1985estimating].
- The last step estimates the effective irradiance incident on a generator subtracting dust and angle of incidence losses from the incident irradiance with the model proposed in [Martin2001].

In figure 4.1 the steps to assess effective irradiation at the plane-of-array is summarized.

4.2.2 Photovoltaic energy yield

Once the effective irradiation that reach solar cells is being assessed, the transformation into power output depends on some factors regarding the photovoltaic system. In order to estimate potential for photovoltaic production, the term yield is defined as the energy produced by the power installed $[\frac{k}{k}]$. That energy, comes from the integration in each time step of the power output of the photovoltaic system.

Considering that reach photovoltaic generator is composed of modules, the generator nominal power output is calculated by multiplying the power output of a module by the number of modules, assuming the same electric performance of all modules.

$$P_{out} = I_m \cdot V_m \quad (4.6)$$

Ambient temperature influence cells performance. The assumption used to this assessment consider a linear relationship between cell temperature and global effective irradiation, Eq.4.7. NOCT in equation 4.7 is considered constant being the temperature of a cell when it works in determined conditions: irradiance of 800 $[\frac{W}{m^2}]$ and ambient temperature of 20°C.

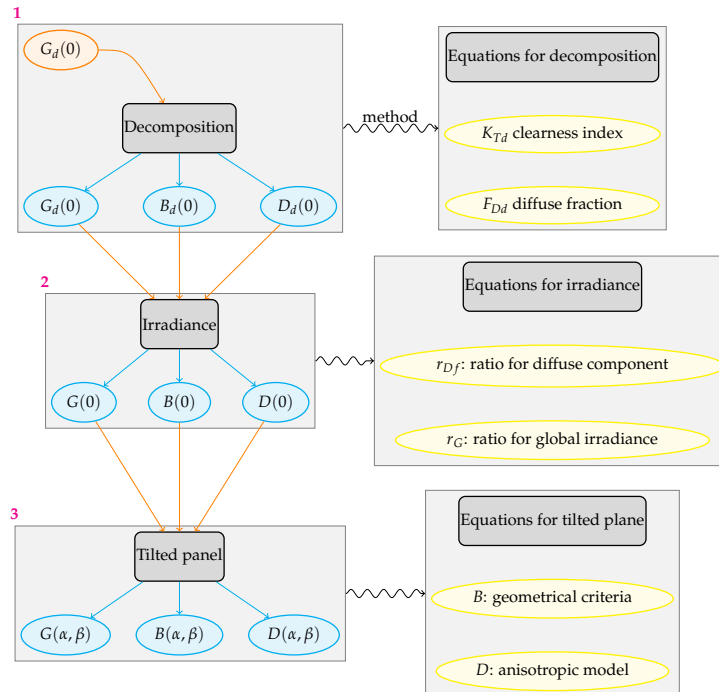


FIGURE 4.1: Algorithm scheme: steps on the calculation of global effective irradiation, incident irradiation at the inclined plane. Orange color means input of the calculation and blue color output or results. If a result in a previous step is used in the next one, arrows linking steps are orange. Right side of the scheme represents the method and equations needed.

$$T_c = T_a + G_{ef} \cdot \frac{NOCT - 20}{800} \quad (4.7)$$

After considering all these factors, the power output of the whole system is assessed by the consideration of a common inverter for transforming DC current into AC, also arrangement losses of the generator are included. Other systems factors that influence the performance of the photovoltaic system are shadows over the generator due to the positions of the PV modules over the land. This factor is not considered in our calculations assuming that we look for an estimation of the potential yield of an area, not the product of a real PV plant. Detailed description of the software employed to the assessment, solaR, is in [Lamigueiro2012]. The process for the photovoltaic output is summarized in table 4.1 including all the steps and elements involved as explained in [Perpinan2009].

4.3 Regional Climate Modeling simulations

4.4 Future projections and scenarios

Element	Method
PV generator	Identical modules with $dV_{oc}/dT_c = 0,475 \frac{\%}{^\circ\text{C}}$ and $NOCT = 47^\circ\text{C}$. The MPP point calculated as in [garcia2005caracterizacio]).
Inverter	<p>Efficiency equation proposed in [jantsch1992results]:</p> $\eta_{inv} = \frac{p_o}{p_o + k_0^o + k_1^o p_o + k_2^o p_o^2} \quad (4.8)$ <p>where $p_o = P_{ac}/P_{inv}$ is the normalized output power of the inverter. The characteristic coefficients of the inverters are: $k_0^o = 0.01$, $k_1^o = 0.025$, $k_2^o = 0.05$.</p>
Other losses	<ul style="list-style-type: none"> • Average tolerance of the set of modules, 3%. • Module parameter dispersion losses, 2%. • Joule losses due to the wiring, 1.5%. • Average error of the MPP algorithm of the inverter, 1%. • Losses due to the MV transformer, 1%. • Losses due to stops of the system, 0.5%.

TABLE 4.1: Calculation procedure for the estimation of energy produced by a PV system from daily global horizontal irradiation data. Left column represents the element of the PV system and the right column the equations and methods used in each case for the efficiency of the elements.

Part III

Results

CHAPTER
5

**LONG-TERM CHARACTERISTICS OF SOLAR RESOURCE OVER THE
IBERIAN PENINSULA**

Abstract

The spatio-temporal characteristics of different renewable resources like solar radiation, wind and precipitation are very different among them and a detailed understanding of each is important for an adequate planning and management of the electricity system. In this chapter, we elaborate a comprehensive methodology to analyse variability and complementarity of PV production that can be applied for long-term energy questions and for climate scales, but it is not limited to those time-scales or to solar resource thanks to the flexibility of the method.

The work is focused on solar irradiation as source of energy for photovoltaic (PV) generation over the Iberian Peninsula, IP, and on photovoltaic productivity, which is defined as the amount of energy generated normalized by the installed capacity at each location. The IP is an interesting site due to the fact that it is a large area with limitations in the interconnectivity with the rest of the European continent. It is also a complex climatic area [] due to its geographical location and its orography, which makes it interesting for testing the methodology.

The main steps of the method are the application of an objective clustering algorithm for performing a regionalization of the whole domain, the analysis of the temporal variability of solar radiation and photovoltaic energy yield, and the intercomparison of the obtained clusters for examining their complementarity.

The approach applied in this chapter means a different perspective to analyse the long-term issues in solar resource as the interannual variability, the influence of the large-scale circulation modes, trends or the synoptic patterns related to its variability. The use of the multi-step scheme allows to simplify the spatial analysis and answer the questions from a more applied point of view.

Data from a satellite dataset of 30 years, which is usually considered as the time for defining a climatology, is used in this chapter and a long-term overview of solar radiation variability is analyzed over the Iberian Peninsula (IP). The spatial distribution and variability of photovoltaic (PV) power yield is calculated for different tracking systems. The variability is analyzed on an interannual time scale, which is relevant for energy supply security and year-to-year price stability. It shows robustness and stability of solar radiation and PV production on average for the whole domain, but with significant differences among clusters that could allow spatial compensation of PV production. The relationship between the variability of solar irradiation and of PV yield is not uniform among the different clusters. Areas where solar irradiation is higher are more sensitive to tracking type.

The whole process described in this chapter provides the information of how solar resource and the PV energy yield perform in a limited area and provide the tools to analyze the relationships between sub-areas and their variability. In this sense, this method can be applied for isolated or nearly isolated electric systems located in regions with a variety of climates, or for interconnected systems involving several countries.

5.1 Introduction

The natural variability of renewable energy resources like solar radiation and wind presents some challenges for the management of electricity systems, which were designed for conventional technologies like nuclear or thermal power plants. For that reason a thorough knowledge and understanding of space-time features of solar radiation is needed. In the case of solar PV energy, its variability Widen2015 can be studied from the perspective of the resource or from the perspective of the PV power output, that includes some aspects of the PV generators involved in variability, like inverters or tilted and tracking panels which increase the complexity of the assessment. There are many studies focused on the short-term variability Zamo.Mestre.ea2014 that analyzed PV production ramps due to changes in solar incident irradiation associated with cloud motion Cros2014, IEA-PVPS-T14-1.32015. Also, the smoothing effect that a well-spread site planning has on the PV production is being investigated Marcos2012, Perpignan.Marcos.ea2013.

Not only short-term scales are important to address renewable resources intermittency but also longer time scales are relevant in order to make the system more efficient and reliable Davy2012. Policymakers, transmission system operators and investment companies, need an accurate evaluation of resources availability in present and future climate conditions for their mid and long-term planning. The analysis of interannual variability has a particular importance in order to assess stability of the resource and the financial viability of renewable energy plants pryor2006inter, as well as the likelihood of strong electricity price oscillations like the ones associated for example with the large interannual variations of hydroelectric production.

Regarding that perspective of long-term variability of solar resources, there are studies focused on long series from stations Sanchez-Lorenzo2009, Sanchez-Lorenzo2013, vazquez2012interannual or reanalysis data that identify low frequency changes in solar radiation, as the “dimming” and “brightening” periods Wild2005, that show relationship between solar irradiation and anthropogenic aerosols Nabat2014a. Some studies examine the influence of large-scale circulation atmospheric modes like the NAO (North Atlantic Oscillation) on solar radiation Pozo-Vazquez2004, Jerez2013, while others study the spatial variability instead of the temporal variability Gueymard.Wilcox2011a.

Some authors make use of regionalization techniques for atmospheric variables in order to analyze them from a climatological point of view Argueso2011 or for solar energy purposes, mainly for operation and short-term assessment Zagouras2013, Zagouras2014, Zagouras.Pedro.2014.

In this chapter a multi-step scheme that systematizes the time-space comparison of solar irradiation or photovoltaic productivity among sub-regions of the target area is described, taking into account a large set of factors involved in PV production that could affect the variability of photovoltaic energy yield. Spatial complementarity between clusters is analyzed through correlation coefficients of solar irradiation and PV energy yield time series, showing possibilities for compensating PV production shortages in certain clusters.

The analysis over the Iberian Peninsula show that most of the results obtain in previous studies can be also seen with this approach. In addition, the methodology allow to give a clearer spatial answer to the questions as well as to sistematize the procedure.

This chapter is organized as follows: in first place, a description of the methodolgy is presented. Each stage of the multi-step scheme is summarized in section ?? and explained in more detail in the Methodology chapter. After that, the clustering algorithm is applied to the irradiation over the Iberian Peninsula and main results are shown.

5.1.1 Methods

The whole comprehensive scheme followed is represented in figure 5.1, showing the 4 stages and procedures that will be explained in detail in the following section.

From data of solar irradiation on the horizontal plane as the starting point of the method, the most common variable obtained from different data sources, the scheme will provide different outputs that can be used to evaluate resource and PV production:

- Regionalization of the area to facilitate the spatial analysis.
- Resource and energy yield aggregated by areas.
- Interannual variability of the resource and the PV production.
- Evaluation of the complementarity of the resource and PV production among areas.

Regionalization by clustering

Regionalization procedures provide the ability of extracting general information of the areas that could be treated as a coherent unit, facilitating the analysis and not considering those characteristics that are not under study. As it was explained in the methodological chapter, classical climatological classifications have some grade of subjectivity due to the fact that they rely on arbitrary assumptions Kottek2006 and their criteria are based on temperature and precipitation trewartha1980koppen. For our purpose, objective and data-derived criteria are more suitable due to the fact that a different variable is analyzed and its classification does not match classical climate divisions. Objective methods based on clustering techniques have been applied successfully over the literature for the analysis of renewable energy resources Polo2015, Zagouras2013, Zagouras2014,

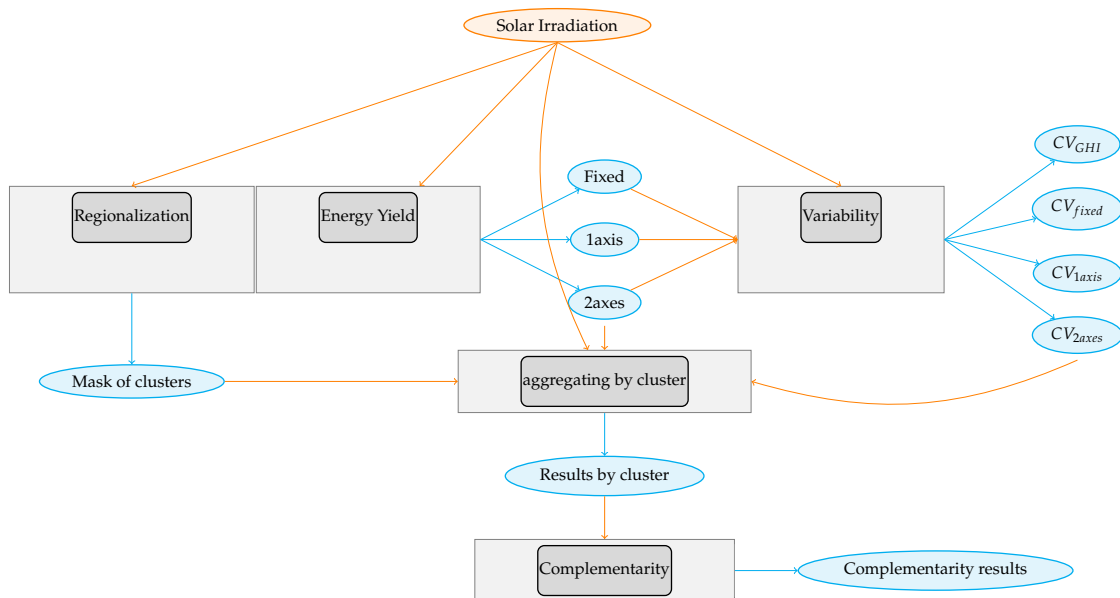


FIGURE 5.1: Scheme: Each gray block represents each of the operations needed to get the variability and complementarity results. Orange ellipses are the data employed and blue ellipses are the results of each stage. If the results of one of the blocks are used as input for another stage, connectors are represented in orange color.

Zagouras.Pedro.2014, gomez2015characterization and atmospheric variables Argueso2011, garcia2012seasonal.

A commonly applied regionalization methodology includes the Kmeans algorithm after preprocessing the data through Principal Component Analysis Ding2004. This two-step method first reduces redundant information by a Principal Component Analysis that decreases dimensionality of the original dataset. After that, k-means algorithm is applied to the reduced data to find the optimal partition of clusters, which is based on similarity between each element or object inside the cluster and its centroid. This is considered as the most representative element of the cluster, and similarity is measured by an objective function defined in the cluster algorithm.

This method presents some problems regarding the random selection of the cluster centroids in the first step. Different initial centroids can lead to different solution or a local optimum could be found. Also, there could be some computational problems if many iterations are needed to get the final partition.

The procedure used in [Argueso2011] and in [Zagouras2014] is adapted to get the optimal partition in our scheme from a combined clustering grouping and avoiding the above mentioned problems: the **k-means partitionational algorithm is initialized with a hierarchical clustering solution of a the dimension-reduced data by a Principal Component Analysis**. For the particular case applied in this work, vectors of daily solar irradiation are used for the regionalization. The following steps are needed to get the optimal partition of clusters in the area:

- **To reduce data dimensionality.** Principal components are eigenvectors of an orthogonal matrix after applied a singular value decomposition (SVD) to the original data, daily solar irradiation vectors, whose initial dimension is reduced to the first eigenvectors that retain 95% of the variance. Considered that, a linear combination of these eigenvectors represents the initial data.
- **Hierarchical clustering to initialize k-means.** A hierarchical clustering method classifies data based on a hierarchy. If it is agglomerative, it will start with a cluster for each observation of the data and observations will group together recursively by similarity using the “complete linkage” method. Once the hierarchy is obtained, centroids can be calculated for each emerged partition with a number of clusters between 2 and n , where n is a high enough selected number of clusters. Centroids will be the initial seed for the Kmeans algorithm, avoiding the computational problems and favoring reproducibility.
- **Kmeans algorithm.** The k-means algorithm is a partitionational clustering method that minimizes an objective function that defines similarity among the elements of each cluster. In our case we made use of the Euclidean distance, Eq. 5.1 between the objects or elements in the cluster and its centroid as the objective function. The number of clusters in which the data is divided into has to be known beforehand. In order to overcome the inconvenience, the algorithm is run from 2 to n clusters and the optimum number is determined by making use of a clustering validity index after that.

$$J = \sum_{i=1}^k \sum_{j=1}^n ||x_i - c_j||^2 \quad (5.1)$$

- **Validity index.** In order to determine the optimal partition, validity clustering techniques are applied. There are two types of validation for the clustering methods. First, external clustering validation that make use of external information out of the data; and secondly, there are internal clustering validation methods that rely only on information from the data 5694060. The latter are used to preserve objectivity as much as possible and are based on two criteria: compactness and separation of the clusters emerged.

We use one of the most applied validity index, the Calinski-Harabasz index CalinskiH, CH, that evaluates the average between and within cluster sums of squares.

- **L-method.** CH index is calculated for every partition from 2 to n clusters. The resulting CH graph in figure 5.2 for the Iberian Peninsula regionalization is shown for a number of clusters between 2 and 70 as an example. Theoretically, the partition with the maximum CH is the optimum, but the graph shows a decreasing trend which leads to imprecision in finding the optimum. The large number of data and the continuous variable analyzed are responsible for that. For that reason, the L-method is applied Salvador2004. This method selects the intersection of two best-fit lines in the graph CH vs. k , where k is the number of clusters of the partition Zagouras2013. All possible pairs of lines that fit linearly to the left and right sequence of data points are created. Each line has at least two points. The total root mean squared error is calculated as in Eq.:5.2:

$$RMSE_T = \frac{c-1}{k-1} RMSE_{left} + \frac{k-c}{k-1} RMSE_{right} \quad (5.2)$$

Where c is the number of clusters where the graph is split into the two fit-lines, k is the total number of clusters. The “total root mean square error” is a weighted error with two terms, one for each side of c in the graph. Each side has a heavier weight depending on the points involved in the fitting. The minimum of $RMSE_T$ gives us the optimum number of clusters of the data Zagouras2013 which are used in the following steps.

Photovoltaic energy yield

The simulation of a photovoltaic energy system is described in a previous chapter. Here it is summarized in order to do not miss the coherence of the text.

The assessment of the power output of a photovoltaic system is carried out in two main steps:

1. In first place, global irradiation on the horizontal plane $G(0)$, which is the most common variable obtained from data sources, has to be transformed into the plane-of-array irradiation, $G(\alpha, \beta)$, where α is

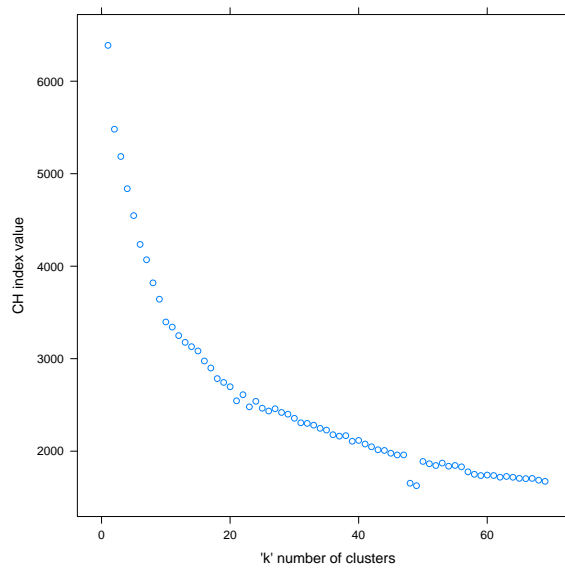


FIGURE 5.2: Calinski-Harabasz index by 'k' number of clusters

the azimuth angle and β the inclination angle of the generator plane. Due to optical losses (reflection, angle of incidence, and dust), the irradiation available is reduced for the photovoltaic cells inside the panels and the plane-of-array irradiation is then denoted as effective irradiation on the PV generator $G_{eff}(\alpha, \beta)$. Three different types of tracking types are considered for the photovoltaic generator that influences on the tilt of the panels:

- **Fixed** panels with an optimum angle of inclination that depends on the latitude of the place.
- **North-South** oriented panels that track the sun daily varying the azimuth angle, we will refer to them as “one axis”
- **Two-axes** tracking system that allows variation of the azimuth and inclination angles, we will refer to them as “two axes”.

2. Once the effective irradiation that reach solar cells has been assessed, second step is the transformation into power output that depends on the photovoltaic system. The photovoltaic system is composed of a PV generator, consisting of several PV modules, and an inverter to transform the DC current output from the generator into AC current to be integrated into the network. In order to estimate potential for photovoltaic production, the term *yield* is defined as the system energy produced divided by the power installed $[\frac{k}{k}]$.

Variability and complementarity

The metric to analyze interannual variability is the coefficient of variation, CV Eq.5.3, which is defined as:

$$CV = \frac{\sigma}{\bar{X}} \quad (5.3)$$

In this equation, σ is the standard deviation of the variable analyzed and it is divided by the mean of the variable in the period of the study. Sometimes CV is represented in percentage. This measure is dimensionless and can be applied in different time scales, which is helpful for comparisons.

To assess complementarity of the solar resource in the area of study, the Pearson's correlation coefficient between the time series of pairs of clusters Eq.5.4 is calculated:

$$\rho_{i,j} = \frac{\sigma_{c_i, c_j}}{\sigma_{c_i} \sigma_{c_j}} \quad (5.4)$$

In this equation, c_i and c_j are the time series corresponding to the clusters i and j . The concept of complementarity is associated with negative correlations between sub-regions of a wider area. If there is such a complementarity, a positive change in the variable for one of the clusters will be associated to a negative change for the other one. This is relevant for identifying spatial compensation possibilities and reducing overall variability in a network with high penetration of solar PV energy.

Complementarity can occur in different scales, either spatial or temporal and to understand it sometimes is a matter of balance. Spatial resolution for the complementarity assessment must be high enough to make sense of the comparison between zones, due to the fact that it is clear that geographically dispersed areas, far from each other, will have very different evolution of atmospheric variables, but may not be interesting from the electricity generation point of view. On the other hand, if the area of study is too small, atmospheric variables and therefore renewable resources will evolve in a very similar way. For such small areas, local complementarity between different resources can be analyzed, but not spatial complementarity of one resource. The methodology presented here addresses this issue by applying the inter-cluster comparison, that ensures

homogeneity within each cluster and differences between them.

Correlation coefficient for a long time series may hide changes in complementarity for shorter sub-periods with higher frequency correlations. For that reason a moving window is applied to the time series calculating the correlation coefficient and providing an indication of how complementarity between clusters varies during the whole period. Width of the window depends on the length of the time-series analysed.

In order to obtain the more important cluster pairs regarding complementarity, the median of the correlation coefficient series is calculated for each pair. After that, the cluster pairs are reordered from lower to higher values of this median correlation.

5.1.2 Results

The optimal partition after having applied the clustering method is represented in figure 5.3. The CH validation procedure gives an optimum number of 19 clusters for the area, where each of the clusters has an homogeneous time evolution of solar irradiation. Due to the nature of clustering techniques, there is not an unique/best method to select the optimum partition. Another index (Davies-Boudin, [**davies1979cluster**]) has been applied for comparison, and the obtained optimum number of clusters was of the same order than for CH index.

Variability and complementarity results

After regionalization, it is performed an analysis of solar irradiation on the horizontal plane and PV yield by tracking system, including their temporal variability.

Regarding interannual variability, we have calculated the CV of two time-aggregated means of solar irradiation and PV yield:

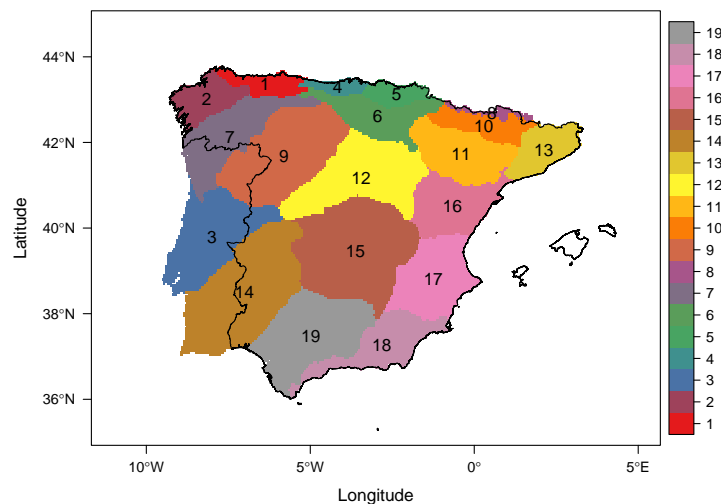


FIGURE 5.3: *Optimal partition of 19 Clusters after applied the algorithm and the validity index*

- On one hand it is applied for the yearly mean of daily irradiation $G_{d,y}(0)$ and yearly PV yield. This metric gives the variation of the of energy from one year to another and if it is low, general stability of the solar resource and PV production is guaranteed.
- On the other hand the interannual variability of the monthly time series $G_{d,m}(0)$ and monthly energy yield is also investigated in order to quantify differences in the annual cycle.

The CV is also aggregated by cluster, in order to facilitate the intercomparison among areas.

Power from the PV generator depends quasi-linearly with solar irradiation at the plane-of-array ($G_{eff}(\alpha, \beta)$), besides second order effects (spectrum, wind, etc) Perpignan2007 . Due to that the fixed typology is the one with lower yield because the amount of irradiation reaching cells is lower than the amount of energy reaching panels when trackers have one or two axes movements.

For areas where solar irradiation is higher, yield differences between trackers are higher. This can be seen in figure 5.4 where yearly mean yield for the 30-years period is aggregated by cluster and tracking system, and clusters are sorted vertically from less to more energy yield. A noteworthy result is that yield increase from fixed panels to one-axis panels is non-linear. This increase ranges between 17% for the clusters with less solar irradiation, located at the northern coast (clusters 4, 5), and 30% for the southern clusters with more solar irradiation (clusters 18, 19). In contrast, energy yield increase from one-axis to two-axes panels is almost constant, around 12% for all clusters. A consequence of the non-linear PV yield increase from fixed to one-axis panels is that the energy yield differences between clusters are much higher for tracking than for fixed systems. While for fixed panels PV energy yield varies between 1000 and 1450 $[\frac{k}{k}]$, for two-axes systems it varies between 1350 and 2100 $[\frac{k}{k}]$. These average values are coherent with results obtained in [Antonanzas-Torres2013] when considering a value of 0.75 for the system performance ratio.

Electricity price variations significantly depend on the variations of the monthly renewable electricity production from year to year. This time-scale is also the most influenced by the large scale circulation modes

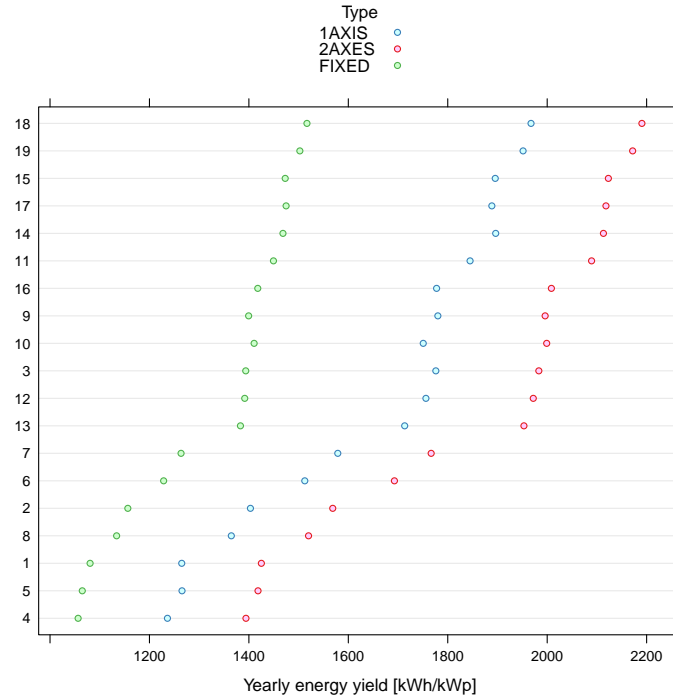


FIGURE 5.4: Yearly mean of PV yield by cluster and for each tracking system $[\frac{k}{k}]$. Values are sort from lower to higher yield values.

for solar potential in the Iberian Peninsula Jerez2013a. The winter half of the year, from October to March, is especially variable.

The interannual variability for monthly yield is higher than for the irradiation at the horizontal plane, as it occurred for yearly values which results are in the appendix. In winter months, these differences in CV are much higher than in summer. This behavior is more pronounced in northern areas.

In order to quantify these differences in variability between solar irradiation and solar power output, the ratio between variability of yield by tracking system and solar irradiation is represented in figure 5.5 for each month and cluster. If CV of energy yield is higher than CV of solar irradiation, values are above one. On the other side values will be below one if CV of solar irradiation is higher than CV of energy yield.

The highest ratios are obtained between CV_{2axes} and CV_{G0} . The ratio of CV_{1axis} is clearly lower in winter months, but is very similar in summer to the ratio of CV_{2axes} . Yield with an 'horizontal' axis tracker and 'two-axes' trackers increase the variability between 20% in summer and more than 80% in some areas in winter. The fixed typology ratio, CV_{fixed}/CV_{G0} has a much wider range in the whole year. In winter months, it has values between 1.2 and 1.6, depending on the cluster, and is not far from the other two typologies. In contrast, this ratio decreases rapidly in summer months, reaching values below one between May and August. This means that for that period, variability of the 'fixed yield' is smaller than variability of solar irradiation at the horizontal plane.

The results of CV show that variability of PV energy yield at tilt panels is higher than variability of solar resource at horizontal plane in most cases, explained by the nature of solar irradiation at tilt panels and its dependency of solar irradiation at horizontal plane, [Perpinan2009].

The monthly time series are also selected for the complementarity analysis.

Regarding solar power complementarity, opposite-evolving time-series for different areas would strongly increase the reliability of the whole electric system, as shortfalls of solar irradiation in certain areas could be compensated by above-normal irradiation in others. However, this ideal situation is difficult to find in a rather

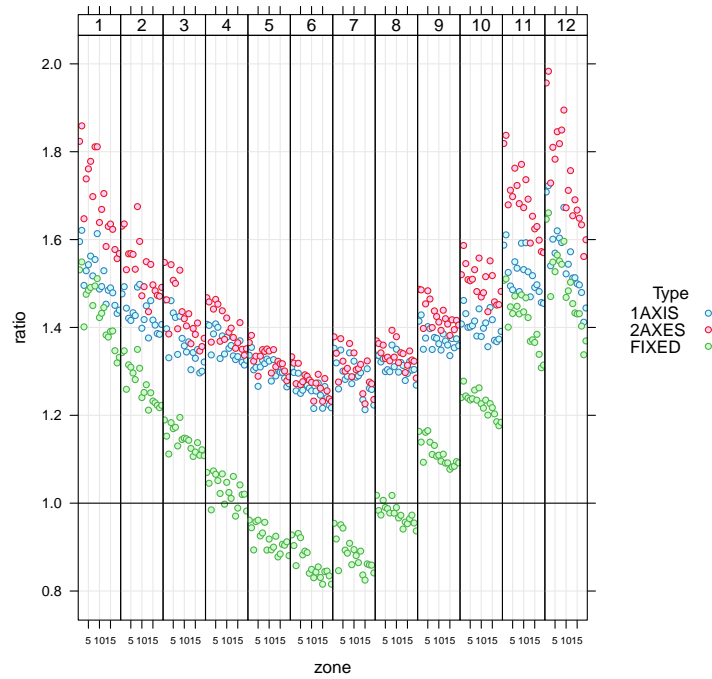


FIGURE 5.5: CV ratios between each type of tracking system and solar irradiation at the horizontal plane, grouped together by month in the graph. Ratios are calculated for each cluster, represented in the x axis. "Fixed" represents $\frac{CV_{fixed}}{CV_{G0}}$, "1 axis" is $\frac{CV_{1axis}}{CV_{G0}}$ and "2 axis" is $\frac{CV_{2axes}}{CV_{G0}}$

limited area like the IP, at least for monthly timescales over a long time period of 30 years. In this case, the absence of correlation becomes also important, as it avoids simultaneous shortfalls or simultaneous above-normal values, and therefore softens the overall power production. The correlation matrix for the 30-year period and each month is in the appendix, showing the results for the whole period. In most cases, the correlation coefficient is highly positive, specially between pairs in the northern part of the Iberian Peninsula. For the southern part, the correlation coefficient is also positive but it decreases in July and August. There are some exceptions between the northern clusters 4 and 5 and the southern clusters 14 to 19, these pairs are only slightly correlated, not correlated or even slightly anticorrelated for some months.

Overall, southern and eastern clusters are uncorrelated at least during part of the year with northern and northwestern clusters. In some cases, the absence of correlation is found between nearby clusters: in winter months, the north-eastern cluster 11 (central Ebro valley) is uncorrelated to the closely-lying clusters 4, 5 and 8 (in the northern coast and Pyrenees). This is probably related to persistent atmospheric situations with north to northwesterly winds, that cause cloudiness in the windward clusters and clear skies in the leeward Ebro cluster, due to a foehn effect. This result points out the selective character of the clustering method.

It could be that the obtained clusters present higher complementarity in shorter sub-periods. We have divided the whole 30-year period in sub-periods of consecutive 15 years. The correlation coefficients have been calculated again for the resulting 15-year moving window, for each pair of clusters and for each month. In this way, we obtain how each correlation coefficient evolves during the 30 year period. The analysis has been applied for the four variables in the study: solar irradiation at the horizontal plane and PV energy yield for each tracking system.

The median value of the correlation coefficient series is calculated for each pair. Each serie comprises 12 monthly values for each of the 15-year moving windows. After that, the cluster pairs are reordered from lower to higher values of this median correlation, and the first 15 pairs (with the lowest median correlation) are selected as the most representative of complementarity. These cluster pairs are represented in figure 5.6, showing the time-evolution of its correlation coefficient. These results are for solar irradiation on the horizontal plane. The corresponding figures for PV yield by tracking system are not shown due to the similar results obtained for this analysis.

The most relevant pairs in terms of complementarity include a northern (1, 2, 4 or 5) and a south-eastern cluster (17 or 18), as can be seen in figure 5.6. The negative correlations for these pairs reach values below -0.6, at least in some 15-year sub-periods. These clusters are negatively correlated in most cases. Clusters 19 and 14 (southern and south-western IP) are also negative correlated with clusters in the north, although with lower values than the south-eastern clusters.

It is important to notice the appearance of cluster pairs 3-4 and 3-5 in this figure. These clusters are closer than the previously commented cases, which highlights the adequacy of the clustering method. All three are Atlantic coast clusters, but while cluster 3 includes part of the western coast, clusters 4 and 5 are northern coast areas. This fact, together with the position of the main mountain ranges, can explain their partially complementary behaviour.

In order to highlight the months with maximum anti-correlation, figure 5.7 presents, for the same 15 cluster pairs as above, the minimum values of the monthly correlation coefficient (where the minimum for each month is calculated over all 15-year sub-periods). Differences between months are clearly observed in this graph. Only two months (March and June) show consistently positive values of this parameter, and therefore a low complementarity. In the other months, this parameter has predominantly negative values, revealing a certain degree of complementarity. July, August and September show rather low values and relatively high complementarity, which is important as these are months with a high productivity and also include the summer demand peak. In general, for the second half of the year, the values of this minimum correlation value are lower than for the first half of the year.

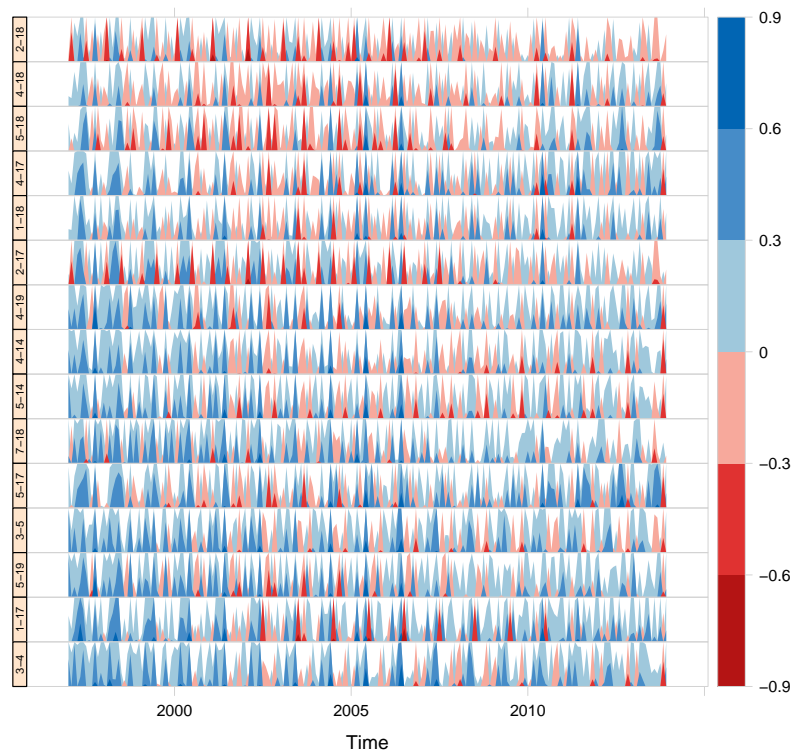


FIGURE 5.6: *Correlation coefficient of solar irradiation at the horizontal plane: evolution of a 15-year moving window of monthly values, for the 15 cluster pairs showing the smallest median correlation values. Monthly negative correlations (in red) and monthly positive correlations (in blue) are represented in the same axis to facilitate the comparison of the multiple time-series. Also, higher correlation values overlap with lower ones, enabling a compact presentation of all the information in a narrower plot. The cluster pairs are indicated on the left, while the year in the x-axis indicates the end of each 15-year moving window.*

5.1.3 Conclusion

5.1.4 Summary

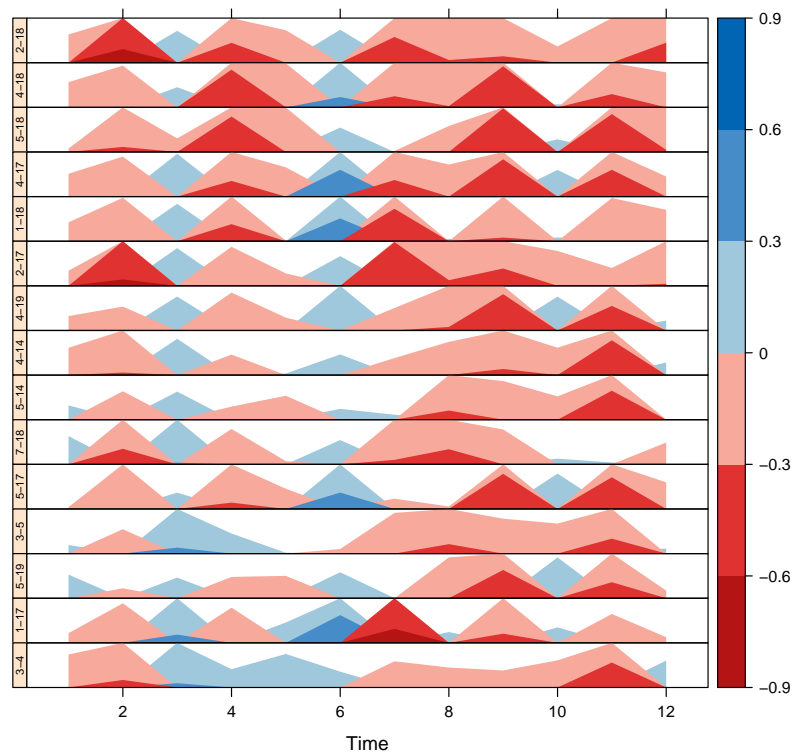


FIGURE 5.7: Correlation coefficient of solar irradiation at the horizontal plane: minimum values of the monthly correlation coefficient, for the same cluster pairs as figure 5.6. The minimum is calculated over all 15-year sub-periods. The type of representation of correlation values is the same as in figure 5.6. The cluster pairs are indicated on the left, while the numbers in the x-axis indicate the months.